Crystal Structure of Chicken Liver Dihydrofolate Reductase Complexed with $NADP^+$ and Biopterin†

Michele A. McTigue,‡ Jay F. Davies, II,‡,§ Bernard T. Kaufman,‖ and Joseph Kraut*,‡

Department of Chemistry, University of California, San Diego, La Jolla, California 92093-0317, and NIDDK, National Institutes of Health, Bethesda, Maryland 20892

Received January 10, 1992; Revised Manuscript Received April 21, 1992

ABSTRACT: The 2.2-Å crystal structure of chicken liver dihydrofolate reductase (EC 1.5.1.3, DHFR) has been solved as a ternary complex with $NADP^+$ and biopterin (a poor substrate). The space group and unit cell are isomorphous with the previously reported structure of chicken liver DHFR complexed with NADPH and phenyltriazine [Volz, K. W., Matthews, D. A., Alden, R. A., Freer, S. T., Hansch, C., Kaufman, B. T., & Kraut, J. (1982) *J. Biol. Chem. 257*, 2528–2536]. The structure contains an ordered water molecule hydrogen-bonded to both hydroxyls of the biopterin dihydroxypropyl group as well as to O4 and N5 of the biopterin pteridine ring. This water molecule, not observed in previously determined DHFR structures, is positioned to complete a proposed route for proton transfer from the side-chain carboxylate of E30 to N5 of the pteridine ring. Protonation of N5 is believed to occur during the reduction of dihydropteridine substrates. The positions of the $NADP^+$ nicotinamide and biopterin pteridine rings are quite similar to the nicotinamide and pteridine ring positions in the *Escherichia coli* DHFR·$NADP^+$·folate complex [Bystroff, C., Oatley, S. J., & Kraut, J. (1990) *Biochemistry 29*, 3263–3277], suggesting that the reduction of biopterin and the reduction of folate occur via similar mechanisms, that the binding geometry of the nicotinamide and pteridine rings is conserved between DHFR species, and that the *p*-aminobenzoylglutamate moiety of folate is not required for correct positioning of the pteridine ring in ground-state ternary complexes. Instead, binding of the *p*-aminobenzoylglutamate moiety of folate may induce the side chain of residue 31 (tyrosine or phenylalanine) in vertebrate DHFRs to adopt a conformation in which the opening to the pteridine binding site is too narrow to allow the substrate to diffuse away rapidly. A reverse conformational change of residue 31 is proposed to be required for tetrahydrofolate release.

The primary physiological role of dihydrofolate reductase (5,6,7,8-tetrahydrofolate:$NADP^+$ oxidoreductase, EC 1.5.1.3, DHFR)[1] is catalysis of the NADPH-dependent reduction of 7,8-dihydrofolate to 5,6,7,8-tetrahydrofolate, derivatives of which function as cofactors in the biosynthesis of thymidylate, purine nucleotides, and other metabolites (Blakely, 1984). The enzymic reduction of other pterins with aliphatic substituents at C6 is also catalyzed by DHFR, although with decreased efficiency (Smith et al., 1987). Of particular biological significance in this regard, the reduction of 7,8-dihydrobiopterin by DHFR is employed in a salvage pathway for the production of 5,6,7,8-tetrahydrobiopterin, the cofactor for the monoxygenases that hydroxylate tyrosine, tryptophan, and phenylalanine (Kaufman, 1967; Kaufman & Fisher, 1973; Abelson et al., 1978; Reinhard et al., 1984; Bowers & Duch, 1988). Vertebrate DHFRs have been shown to reduce dihydrobiopterin at rates ranging from 2.7% (bovine liver DHFR; Smith et al., 1987) to 50% (chicken liver DHFR; Kaufman, 1967) of the rate of dihydrofolate reduction. Reduction of biopterin to dihydrobiopterin is also catalyzed by chicken liver DHFR at low pH, although at less than 1% of the rate of dihydrobiopterin reduction (Kaufman, 1967). The chemical structures of folate and biopterin are shown in Figure 1.

Since DHFR is a target for both antineoplastic and antimicrobial agents, it has been intensively studied for many years. For reviews of the extensive literature pertaining to DHFR, see Blakely (1984), Friesheim and Matthews (1984), and Kraut and Matthews (1987). Full kinetic pathways have been established for DHFR from *Escherichia coli* (Fierke et al., 1987), *Lactobacillus casei* (Andrews et al., 1989), mouse (Thillet et al., 1990), and human (Appleman et al., 1990), and the crystal structures of a variety of substrate, cofactor, and inhibitor complexes have been determined for DHFR from *E. coli* (Bolin et al., 1982; Filman et al., 1982; Bystroff et al., 1990, 1991), *L. casei* (Bolin et al., 1982; Filman et al., 1982), chicken liver (Volz et al., 1982; Matthews et al., 1985a,b), L1210 mouse lymphoma (Stammers et al., 1987), S180 mouse sarcoma (Groom et al., 1991), human (Oefner et al., 1988; Davies et al., 1990), and type II resistant-plasmid R67 of *E. coli* (Matthews et al., 1986). Refer to Table I for a summary of some relevant crystallographic statistics for all reported structures of DHFRs from vertebrate sources. The crystal structure of chicken liver DHFR in ternary complex with $NADP^+$ and biopterin, which is the subject of this paper, was initially solved in our laboratory to a resolution of 2.8 Å (D. A. Matthews, unpublished results). We present here the refined 2.2-Å structure of this complex, which still remains the only reported structure of a vertebrate DHFR complexed with both substrate and cofactor.[2] Analysis of this higher resolution structure has shed some further light on a possible

† This work was supported by USPHS Training Grant GM07313 and by NIH Grant CA 17374 to J.K.

* Author to whom correspondence should be addressed.

‡ University of California, San Diego.

§ Present address: Agouron Pharmaceuticals, 3565 General Atomics Ct., San Diego, CA 92121.

‖ National Institutes of Health.

[1] Abbreviations: DHFR, dihydrofolate reductase; hDHFR, recombinant human DHFR; cDHFR, chicken liver DHFR; ecDHFR, *Escherichia coli* DHFR; $NADP(^+/H)$, nicotinamide adenine dinucleotide phosphate (oxidized/reduced); pABG, *p*-aminobenzoylglutamate; F_o, observed structure factor; F_c, calculated structure factor; α_c, calculated phases; *B*-factor, atomic temperature factor.

0006-2960/92/0431-7264$03.00/0

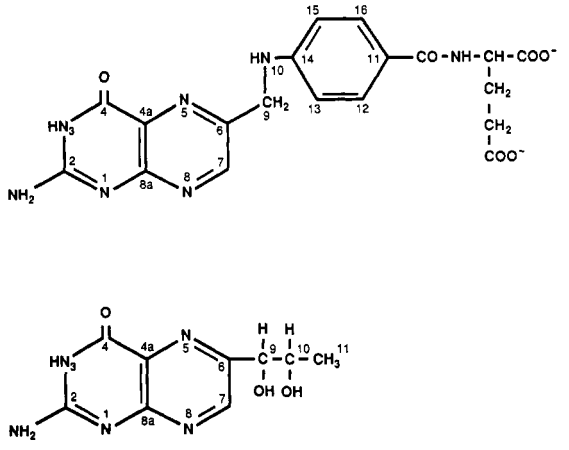

FIGURE 1: Covalent structure and atomic numbering for folate (A) and biopterin (B).

mechanism of substrate protonation and on the possible catalytic function of the *p*-aminobenzoylglutamate moiety of folate substrates.

MATERIALS AND METHODS

Chicken dihydrofolate reductase (cDHFR) was purified as described previously (Kaufman & Kemerer, 1977). Crystals of the cDHFR·NADP$^+$ binary complex were grown by a procedure similar to that reported for the NADPH holoenzyme complex (Volz et al., 1982). A 200-μL aliquot of a solution containing 15 mg/mL cDHFR, 2 mM NADP$^+$ (Sigma Chemical), 10 mM calcium acetate, 2 mM dithiothreitol, and 20 mM Tris-HCl at pH 7.5 was placed in a 1-mL glass beaker and allowed to equilibrate by vapor diffusion with a reservoir solution containing 23% (v/v) ethanol, 10 mM calcium acetate, and 20 mM Tris-HCl at pH 7.5 and 4 °C. Large crystals (on average 1.0 × 0.5 × 0.2 mm) appeared within 3 days. Ternary cDHFR·NADP$^+$·biopterin crystals were obtained by soaking cDHFR·NADP$^+$ binary crystals for 24 h in a solution containing 40% (v/v) ethanol, 20 mM Tris-HCl, 10 mM calcium acetate, 2 mM dithiothreitol, 1 mM NADP$^+$, and a saturating concentration of L-*erythro*-biopterin (Fluka Chemical) at pH 7.5. These ternary crystals, which are isomorphous with the NADPH holoenzyme crystals, belong to space group *C*2 with a = 89.44 Å, b = 48.31 Å, c = 64.26 Å, and β = 125.1°.

X-ray diffraction data to a Bragg spacing of 2.2 Å were collected from one crystal at ambient temperature (~20 °C) using the UCSD Mark III multiwire area detector (Cork et al., 1973; Xuong et al., 1985). The data were processed with programs developed at the UCSD facility (Anderson, 1987) to an R_{sym}[2] of 0.022, based on an average of three observations per unique reflection. The data set of 10 688 unique structure factors contains 91.2% of the data to 2.2-Å resolution.

The presence of biopterin in the crystal structure was confirmed by calculating a difference Fourier with coefficients $(F_{o(ternary)} - F_{o(NADPH)}),\alpha_c$ using the observed structure factors $[F_{o(NADPH)}]$ and calculated phases (α_c) from the refined 1.8-Å cDHFR·NADPH structure (S. J. Oatley, unpublished results; Brookhaven PDB entry = 8DFR). Maps were inspected on a Silicon Graphics Iris 2400 workstation with the molecular modeling programs Frodo (Jones, 1978) and MMS (Dempsey, 1987). The most prominent feature in the map is a large piece of continuous positive electron density (8σ) in the substrate binding site into which biopterin was easily fitted. Near the biopterin density were positive and negative peaks (4σ) close to the side chains of residues E30, Y31, and F34. As most changes indicated by this difference Fourier were consistent with the previously determined 2.8-Å cDHFR·NADP$^+$·biopterin structure, the latter was used as a starting model for refinement against the higher resolution data. Least-squares refinement was performed on the San Diego Supercomputer Center Cray X-MP/48 with a local version of the program PROLSQ (Konnert, 1976; Hendrickson, 1981) which incorporates a correction for X-ray scattering by amorphous solvent (Bolin et al., 1982). Refinement was initiated using all data out to 2.2 Å. Throughout refinement, individual atomic temperature factors were refined for all atoms while occupancy factors were held constant. In addition to atomic distance restraints, planar restraints were applied to atoms in peptide bonds, aromatic side chains, the pteridine ring of biopterin, and the adenine and nicotinamide rings of NADP$^+$. The 3′-carboxamide substituent and the pyridine ring of the nicotinamide were restrained to be coplanar as the density for these atoms in $(F_o - F_c),\alpha_c$ omit maps appeared to lie in a single plane, and the nicotinamides of other DHFR–coenzyme complexes have their carboxamide coplanar with the pyridine ring (Filman et al., 1982; Volz et al., 1982; Bystroff et al., 1990). The ratio of structure factor observations to adjustable parameters was 1.6. When refinement reached convergence, both $(F_o - F_c),\alpha_c$ and $(2F_o - F_c),\alpha_c$ Fourier maps were inspected. Atoms that could not be modeled into interpretable density were removed, the remainder of the model was refined to convergence, and difference Fourier maps were again examined. Solvent atoms were modeled where isolated peaks in the difference maps were greater than 3 σ, were within 2.4–3.2 Å of a heteroatom, and suggested reasonable hydrogen-bonding geometry.

A total of 23 cycles of restrained least-squares refinement were performed resulting in an *R*-factor[3] of 0.14 for all data to 2.2-Å resolution, a root mean square (rms) deviation in bond lengths of 0.021 Å from their dictionary values, and an rms deviation of atoms from their least-squares plane of 0.023 Å. These statistics correspond to an estimated mean uncertainty in atomic positions of 0.1 Å (Luzatti, 1952). The model consists of 1489 protein, 17 biopterin, 48 cofactor, and 132 solvent atoms with average temperature factors (*B*-factors) of 22.7, 12.0, 11.3, and 45.7 Å^2, respectively. The C-terminal residues 187–189 and parts of the side chains of R2, K80, E104, and K178 are not modeled owing to uninterpretable electron density.

RESULTS

Protein and Cofactor Conformation. The folding of cDHFR in the ternary NADP$^+$·biopterin complex, depicted in Figure 2, is essentially identical to that of the cDHFR·NADPH and the hDHFR·folate structures. As this folding geometry has been described in detail (Davies et al., 1990), only a brief

2

$$R_{sym} = \frac{\sum_{hkl}\sum_i |I_i - \bar{I}|}{\sum_i I_i}$$

where I_i is the intensity of the ith observation of reflection (hkl) or a symmetry-related reflection and $\bar{I}$ is the scaled mean intensity. The summation is over all measured reflections.

3

$$R = \frac{\sum_{hkl}|F_o - F_c|}{\sum_{hkl}F_o}$$

The summation is over all measured reflections (hkl).

Table I: Crystal Structures of DHFR from Vertebrate Sources

species	complex	space group	*a* (Å)	*b* (Å)	*c* (Å)	α	β	γ	resolution (Å)	*R* (%)	reference
chicken liver	phenyltriazine·NADPH	*C2*	89.0	48.3	64.0	90	125.2	90	2.9		Volz et al. (1982)
	trimethoprim·NADPH	*C2*	89.0	48.3	64.0	90	125.2	90	2.2	21	Matthews et al. (1985a)
	inhibitors·NADPH	*C2*	89.0	48.3	64.0	90	125.2	90	2.2		Matthews et al. (1985b)[a]
	apo	*C2*	89.2	47.6	60.0	90	125.4	90	3.0	23	D. A. Matthews (unpublished results)[b]
	NADPH	*C2*	89.1	48.0	64.3	90	124.8	90	2.0	22	Matthews et al. (1985a)
	NADPH	*C2*	89.1	48.0	64.3	90	124.8	90	1.8	21	S. J. Oatley (unpublished results)[c]
	biopterin·$NADP^+$	*C2*	89.4	48.3	64.3	90	125.1	90	2.2	14	this report
recombinant human	folate	*R3*	86.3	86.3	77.0	90	90	120	2.0	19	Oefner et al. (1988)
	trimethoprim	*R3*	86.3	86.3	77.0	90	90	120	3.5		Oefner et al. (1988)
	methotrexate	*R3*	86.3	86.3	77.0	90	90	120	3.5		Oefner et al. (1988)
	folate	*P1*	36.1	38.7	76.9	94.3	91.7	110.0	2.3	18	Davies et al. (1990)
	5-deazafolate	*P1*	36.1	38.7	76.9	94.3	91.7	110.0	2.3	18	Davies et al. (1990)
mouse L1210	trimethoprim·NADPH	$P2_1$	43.7	61.6	41.9	90	116.3	90	2.0	18	Stammers et al. (1987)
	methotrexate·NADPH	$P2_1$	43.7	61.6	41.9	90	116.3	90	2.5	19	Stammers et al. (1987)

[a] Structures of 10 complexes with triazine and pyrimidine inhibitors. [b] Briefly described in a review article by Kraut and Matthews (1987). [c] Available from the Brookhaven Protein Data Bank under identification code 8DFR.

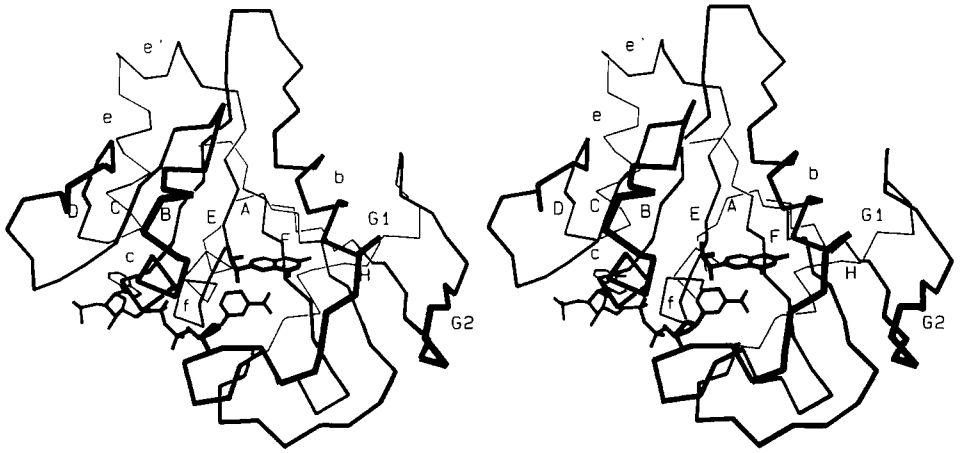

FIGURE 2: α-Carbon representation of chicken liver dihydrofolate reductase complexed with $NADP^+$ and biopterin. β-Strands are labeled with upper case letters and α-helices with lower case.

overview will be given here. The main structural element of cDHFR is an eight-stranded twisted β-sheet composed of seven parallel strands and one carboxy-terminal antiparallel strand. The remainder of the protein comprises five α-helices, one left-handed polyproline-like helix, eight tight turns, and several extended loops.

$NADP^+$ is bound in an extended conformation similar to that previously reported for cofactor binding to DHFR, with nearly all the protein–cofactor interactions involving conserved residues (Matthews et al., 1979; Filman et al., 1982; Volz et al., 1982; Bystroff et al., 1990). Since there are slight differences in the interactions between cDHFR and cofactor observed in this cDHFR·$NADP^+$·biopterin complex from those described for the 2.9-Å cDHFR·NADPH·phenyltriazine structure (Volz et al., 1982), a list of these interactions is given in Table II. These apparent differences are probably due to the increased resolution and refinement of the structure reported here as compared with the 2.9-Å cDHFR·NADPH·phenyltriazine structure. Indeed, protein–cofactor interactions are identical in this cDHFR·$NADP^+$·biopterin structure and the 1.8-Å cDHFR·NADPH structure (S. J. Oatley, unpublished results; Brookhaven PDB entry 8DFR).

The nicotinamide ring is bound near the center of the molecule in a cleft formed by the divergence of βE and βA. A conserved cis-peptide between G116 and G117, which terminates βE and begins αF, creates a curve in the backbone of residues 115–117 that accommodates the N1–C6–C5–C4 edge of the nicotinamide ring. The space between this cis-peptide and A9, at the C-terminus of βA, is large enough to allow the nicotinamide ring to lie parallel with the β-sheet. In this position, the accessible ring CH groups make closer than van der Waals contact with four protein oxygens situated along the perimeter of the pyridine ring, the dipoles of which may help to stabilize a positively charged nicotinamide ring in the transition state (Filman et al., 1982). The B-side of the nicotinamide faces the interior of the protein where it packs against the side chains of I16 and Y121, while the A-side is directed toward the opening of the nicotinamide binding site. In binary complexes with cofactor, the A-side of the nicotinamide ring is exposed to the bulk solvent, while in the cDHFR·$NADP^+$·biopterin complex it is shielded by the pyrazine ring of biopterin.

Three hydrogen bonds to the protein induce the 3′-carboxamide group to lie approximately in the plane of the pyridine ring with the carboxamide carbonyl syn to C4 of the pyridine [τ(C4–C3–C7–O7) = 5°]. The carboxamide NH_2 group hydrogen-bonds to the backbone oxygens of A9 and I16, while the carboxamide carbonyl hydrogen-bonds to the backbone nitrogen of A9.

Biopterin Binding Site. As shown in Figure 3, the pteridine ring of biopterin binds in a cavity formed by atoms in the backbone of residues 7–9 (βA) and 115 (βE), the side chains of residues E30, Y31, and F34 (αB), the side chains of L22 and W24 (polyproline helix), and the nicotinamide of $NADP^+$.

Table II: Interactions between NADP+ and Chicken Liver Dihydrofolate Reductase

NADP+ component[a]	DHFR residue	interaction type
adenine	1.75 side chain	hydrophobic
	S92 backbone	hydrophobic
	S119 side chain	hydrophobic
	V120 side chain	hydrophobic
adenine mononucleotide ribose	K54 backbone	hydrophobic
	K54 amino	charge interaction with 2′-phosphate
	K55 amido	H bond to AO5′
	L75 backbone	hydrophobic
	S76 backbone	hydrophobic
	R77 backbone amido	H bond to 2′-phosphate
	R77 guanidinium	charge interaction with 2′-phosphate via water-393
pyrophosphate	T56 amido	H bond to AO2P
	T56 hydroxyl	H bond to AO2P
	K55 amino	charge interaction with NO2P via water-814
	K55 side chain	hydrophobic
	G117	hydrophobic
	G117 amido	H bond to AO1P
	S118 amido	H bond to NO1P
	S118 side chain	H bond to NO1P via water-318
	T146 side chain	H bond to NO2P via water-814
nicotinamide mononucleotide ribose	D21 carbonyl	H bond to NO2′ and NO3′
	D21 amido	H bond to NO3′
	T56 side chain	hydrophobic
	I16 backbone	hydrophobic
	G2O	hydrophobic
	G117	hydrophobic
	T146 side chain	hydrophobic
nicotinamide	V8 backbone	hydrophobic
	I16 side chain	hydrophobic
	I16 carbonyl	H bond to NN7
	A9 amido	H bond to NO7
	A9 carbonyl	H bond to NN7
	L22 side chain	hydrophobic
	W24 side chain	hydrophobic
	I16 carbonyl	dipole with NC2
	Y121 hydroxyl	dipole with NC4
	V115 carbonyl	dipole with NC5
	T56 hydroxyl	dipole with NC6
	pyrazine of biopterin	hydrophobic

[a] Atomic designations for NADP+ as given in Bystroff et al. (1990).

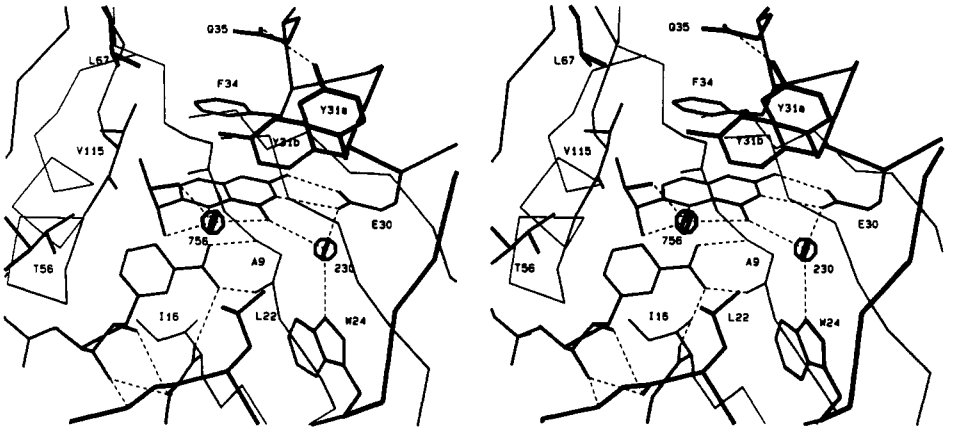

FIGURE 3: Catalytic site of chicken liver dihydrofolate reductase complexed with NADP+ and biopterin. Hydrogen bonds are depicted as dashed lines, and water molecules are displayed as spheres. For clarity, only side chains which directly contact NADP+ or biopterin are shown.

These amino acid residues are conserved in all reported vertebrate DHFR sequences with the exception of Y31, which is a phenylalanine in all other vertebrate sequences. The side-chain carboxylate of E30 is hydrogen-bonded to both N3 and the 2-amino groups of the pteridine ring. The biopterin and cofactor are bound such that the pteridine and nicotinamide rings are tilted by approximately 45° relative to one another, with extensive van der Waals contacts occurring between the biopterin pyrazine ring and the O7–C7–C3–C4 fragment of the nicotinamide. Not surprisingly, the closest approach (3.3 Å) occurs between the nicotinamide hydride donor atom (C4) and the pteridine hydride acceptor atom of biopterin (C7). The distance between C4 of the nicotinamide and the atom (C6) that would be the hydride acceptor in the case of dihydropteridines is 3.5 Å.

The biopterin dihydroxypropyl group is bound with an OH9–C9–C10–OH10 torsion angle (τ) of 71°. The geometry of the substrate binding site requires that the dihydroxypropyl substituent curl back toward the pteridine [τ(C6–C9–C10–C11) = 65°], since in a more extended conformation the terminal methyl group (C11) of the substituent would be too close to the side chain of I16. As it is bound, this methyl

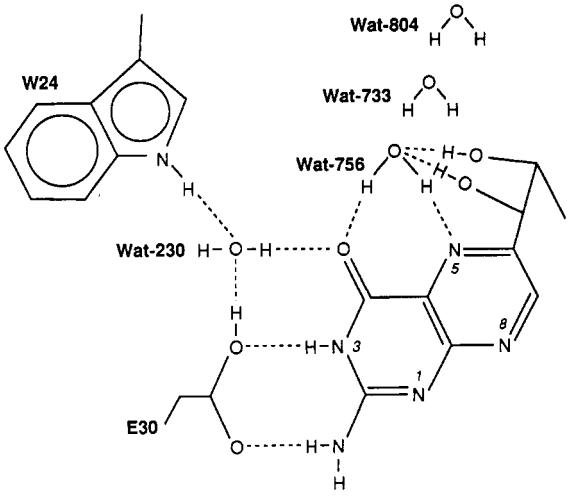

FIGURE 4: Schematic diagram showing potential hydrogen bonds involving biopterin. Water-733 and water-804 are part of the solvent channel connecting water-756 with the protein surface.

group is in contact only with C6 of the pteridine ring. Both hydroxyls of the dihydroxypropyl group are hydrogen-bonded to water-756, a water molecule not previously observed in any other DHFR structure, which is also hydrogen-bonded to both O4 and N5 of the pteridine (see Figures 3 and 4). In addition, one of the hydroxyls (OH9) is hydrogen-bonded to water-648 which in turn is hydrogen-bonded to the 2′-hydroxyl of the nicotinamide ribose. Water-648 is also present in the cDHFR·NADPH structure, and its position does not seem appreciably altered by interaction with the dihydroxypropyl group. The only contact the dihydroxypropyl group makes with the protein is a hydrophobic interaction between C9 and the side chain of T56.

A series of ordered water molecules links the bound pteridine of biopterin with the bulk solvent. One solvent channel, borderd by residues 22–30, has its terminal water (water-230) hydrogen-bonded to the side-chain carboxylate of E30, the indole of W24, and O4 of biopterin. Water-230, a conserved water present in all DHFR structures, corresponds to water-401 in the human DHFR·folate structure (Davies et al., 1990) and water-206 in the ecDHFR·$NADP^+$·folate structure (Bystoff et al., 1990). The other solvent channel, bordered by the side chain of Y31 and the loop of residues 59–61, connects the bulk solvent to the pteridine through the new water molecule, water-756. As noted above, this water makes four hydrogen bonds with biopterin (Figure 4). With the exception of the 2.2-Å separation of water-756 and OH10, which is too close for a normal hydrogen bond (but see below), all of these hydrogen bonds possess reasonable geometry. Since the position of water-756 corresponds to that of a water molecule which we have previously suggested may bind transiently during the reduction of dihydrofolate (Bystroff et al., 1990) but which is not present in the known structures of DHFR complexed with folate, it is of special interest. Therefore, a test was performed to verify that the density assigned to water-756 is not due to an alternate conformation of the biopterin dihydroxypropyl group. Both water-756 and the biopterin were removed from the model, and two cycles of refinement were computed. The resulting omit map, contoured at 5σ, contained positive electron density coincident with the position of water-756 that was distinct from the density of bound biopterin. It was found that a 12° rotation of the C6–C9 bond, from the position determined by least-squares refinement, results in a more reasonable OH10 to water-756 separation of 2.8 Å while leaving all atoms of the dihydroxypropyl group in well-defined density. Since the temperature factor of water-756 is relatively high (B = 39 Å^2), it is likely that the dihydroxypropyl tail occupies two slightly differing conformations, one of which precludes water-756 binding.

The side chain of Y31, which flanks the water-756 binding pocket, also occupies two distinct conformations. In one conformation (Y31a, 30% occupancy), which is similar in position to Y31 in the cDHFR·NADPH complex, its side chain is hydrogen-bonded to the side-chain amide of Q35, and in the second orientation (Y31b, 70% occupancy), this side chain forms parts of the pteridine and water-756 binding sites. The two side-chain positions of Y31 differ by approximately a 60° rotation about the Cα–Cβ bond. Conformational changes in the Y31 side chain have also been observed upon inhibitor binding to cDHFR (Volz et al., 1982; Matthews et al., 1985a,b).

Comparison with the cDHFR·NADPH Complex. Protein conformational changes that accompany biopterin binding to the holoenzyme were analyzed by comparing the biopterin ternary complex structure with the isomorphous 1.8-Å cDHFR·NADPH complex structure. The binding of biopterin to the holoenzyme complex appears to have only a negligible effect on the protein backbone as the rms deviation in equivalent Cα positions between the two complexes is only 0.2 Å, with the largest deviation in a Cα position of 0.6 Å at the carboxy-terminal residue V186. There is, however, an apparent decrease in protein mobility as indicated by a decrease in the average B-factor from 35 Å^2 in the holoenzyme to 22 Å^2 in the biopterin ternary complex.

The largest differences between the binary NADPH and ternary $NADP^+$·biopterin structures occur at the side chains of residues E30 and Y31. The side-chain carboxylate of E30 is significantly stabilized by a pair of hydrogen bonds to N3 and the 2-amino group of biopterin, as evidenced by a decrease in its average temperature factor from 74 Å^2 in the NADPH complex to 9 Å^2 in the ternary complex. Though this ordering is accompanied by a 0.9-Å movement of the carboxylate side chain, its high temperature factor in the holoenzyme complex indicates that its position is ill-defined in that structure. Associated with the stabilization of E30 is an increase in the ordering of water-230, which is hydrogen-bonded to the side-chain carboxylate of E30 and the indole nitrogen of W24. The B-factor for this water is 47 Å^2 in the NADPH complex and 12 Å^2 in the ternary biopterin complex. As noted above, the side chain of Y31 occupies a single position in the holoenzyme but two distinct positions in the ternary complex. Since one of the two orientations in the ternary complex (Y31a) is equivalent to that in the holoenzyme structure, two explanations seem plausible: either the side chain of Y31 actually does occupy two conformations when biopterin is bound or the biopterin site is only partially occupied. However, the low average temperature factor of biopterin (12.0 Å^2), obtained with refinement performed assuming full occupancy, suggests that the former explanation is more likely. Also, there is no negative density surrounding the biopterin molecule in the final $(F_o - F_c),\alpha_c$ difference map that would imply that the occupancy factor of 1.0 for biopterin is too high.

The only significant deviation between the position of NADPH in the binary complex and $NADP^+$ in the ternary complex occurs for the nicotinamide ring (Figure 5). It seems that both the presence of bound biopterin and the oxidation state of the cofactor affect the nicotinamide position. The difference in nicotinamide positions between the two complexes

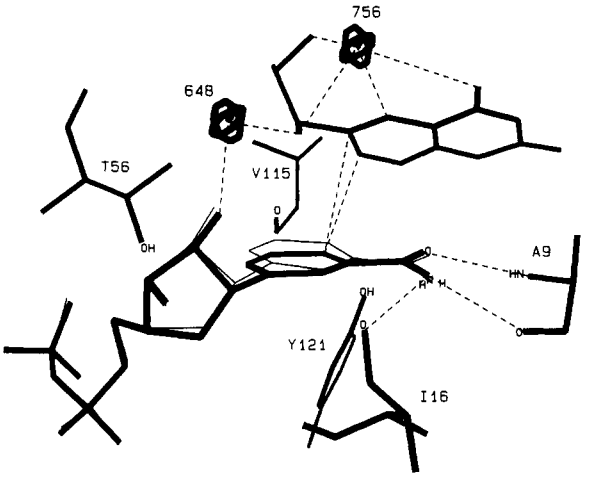

FIGURE 5: Nicotinamide binding site of the cDHFR·NADP+·biopterin structure superimposed with the coordinates of NADPH (thin lines) from the 1.8-Å cDHFR·NADPH complex structure (S. J. Oatley, unpublished results; Brookhaven PDB entry = 8DFR). Hydrogen bonds are depicted by dashed lines, and water molecules are depicted as spheres.

is best described as a 9° rotation about an axis approximately collinear with the nicotinamide C2–C3 bond so that in the ternary complex the N1–C6–C5–C4 nicotinamide fragment binds 0.3–0.4 Å further away from the pteridine binding site. The nicotinamide appears to rotate on ternary complex formation to avoid close contact between C4 (nicotinamide) and both C6 and C7 (pteridine). If this rotation did not occur, the separations between C4 (nicotinamide) and C6 and C7 (pteridine) would be 3.1 and 3.0 Å, respectively, rather than the more reasonable 3.5 and 3.3 Å observed in the NADP+·biopterin structure. The predicted van der Waals distance between C4 (NADP+) and either C6 or C7 (pteridine) is 3.5 Å (Bondi, 1964). It is also possible that the differing oxidation states of the nicotinamide rings contribute to the difference between their positions in the two complexes. For example, as bound to cDHFR, the *pro-S* hydrogen of the reduced nicotinamide ring of NADPH contacts the hydroxyl of Y121, which lies on the opposite face of the nicotinamide from biopterin (Figure 5). The observed decrease in the separation between this hydroxyl and C4 (nicotinamide) from 3.4 Å in the holoenzyme to 3.2 Å in the NADP+·biopterin complex, if real, might result from the absence of this hydrogen in NADP+.

Comparison of Pteridine Binding in Biopterin and Folate Complexes. For a comparison of the binding of biopterin and folate to DHFR, the hDHFR·folate (Davies et al., 1990) and ecDHFR·NADP+·folate (Bystroff et al., 1990) structures were superimposed onto the cDHFR·NADP+·biopterin structure using the least-squares superpositioning program OVRLAP (Rossman & Argos, 1975). Of the two molecules in the asymmetric unit of the hDHFR crystals, molecule 2 was chosen for the comparison as it is the more well-ordered. Residues 1–3 and 186 of the cDHFR were removed from the coordinate set as the corresponding residues are disordered in the hDHFR structure. Similarly, residues which correspond to sequence insertions between ecDHFR and cDHFR, according to the alignment of Freisheim and Matthews (1984), were removed from the coordinate sets before least-squares superpositioning. The resulting differences in Cα positions from those in the cDHFR structure were 0.6 Å for the hDHFR structure (182 common Cα's) and 1.8 Å for the ecDHFR structure (152 common Cα's). The largest differences (1.2–1.8 Å) between the cDHFR and hDHFR structures occur near lattice contacts, and the largest differences (3–6 Å) between cDHFR and ecDHFR occur adjacent to sequence insertions.

While the protein conformation is more similar between the ternary cDHFR·NADP+·biopterin complex and the binary hDHFR·folate complex than between the ternary cDHFR and ternary ecDHFR·NADP+·folate complexes, the position of the substrate pteridine ring is nearly identical in the two ternary complexes while in the binary hDHFR complex the pteridine ring is rotated relative to this position. As Figure 6 shows, the pteridine positions of the ternary cDHFR and binary hDHFR complexes differ by approximately at 20° rotation about an axis collinear with the C4A–N5 pteridine bond such that the pteridine ring of the hDHFR·folate complex extends approximately 1 Å deeper into the catalytic site. The positions of the cofactor nicotinamide rings are also nearly coincident in the ternary cDHFR and ecDHFR structures; therefore, the geometrical relationship between the nicotinamide and pteridine rings is also quite similar in these two complexes. More specifically, the C4 (nicotinamide) to C6 and C7 (pteridine) distances are 3.3 and 3.1 Å, respectively, in the ecDHFR complex and 3.5 and 3.3 Å for the cDHFR complex.

DISCUSSION

Substrate–Cofactor Geometry. The close agreement of the pteridine–nicotinamide geometry between the cDHFR·NADP+·biopterin and ecDHFR·NADP+·folate complexes suggests that (1) the relative binding geometry of the nicotinamide and pteridine moieties is a conserved feature of DHFR catalytic sites, (2) the pABG of folate does not significantly affect the pteridine position in these ground-state complexes, and (3) the reduction of biopterin and folate most likely occurs via the same mechanism. Further, the precise geometrical relationship between substrate or cofactor and the surrounding enzyme appears to depend more on the ligation state (binary versus ternary) than upon the species of DHFR. The pteridine positions in the ternary cDHFR·NADP+·biopterin and ecDHFR·NADP+·folate complexes are nearly identical despite the smaller size of ecDHFR (159 amino acids) as compared with cDHFR (189 amino acids) and the significant structural differences between the bacterial and vertebrate enzymes (Matthews et al., 1985a,b; Davies et al., 1990), while the pteridine rings of the cDHFR·NADP+·biopterin and hDHFR·folate complexes are rotated relative to one another even though hDHFR (186 amino acids) and cDHFR are similar in size and have a sequence identity of 75%. Similarly, in the binary cDHFR·NADPH complex, the nicotinamide ring is inserted 0.3–0.4 Å more deeply into the pteridine substrate binding site than it is in the cDHFR·NADP+·biopterin complex, despite the near-identity of the enzyme conformations in these isomorphous crystal structures.

This dependence of precise binding geometry upon the ligation state of DHFR supports and extends our previous hypothesis that the enzyme employs slightly overlapping pteridine and nicotinamide binding sites to stabilize the sub van der Waals hydride donor–hydride acceptor separation required in the transition state (Davies et al., 1990). For a model reaction represented by the reduction of methyleniminium cation by 1,4-dihyropyridine, the theoretically calculated ideal hydride donor–hydride acceptor separation is 2.6 Å (Wu & Houk, 1987). Superposition of the hDHFR·folate and cDHFR·NADPH binary complexes yielded a 2.5-Å separation between the hydride donor atom (C4 nicotinamide) and the

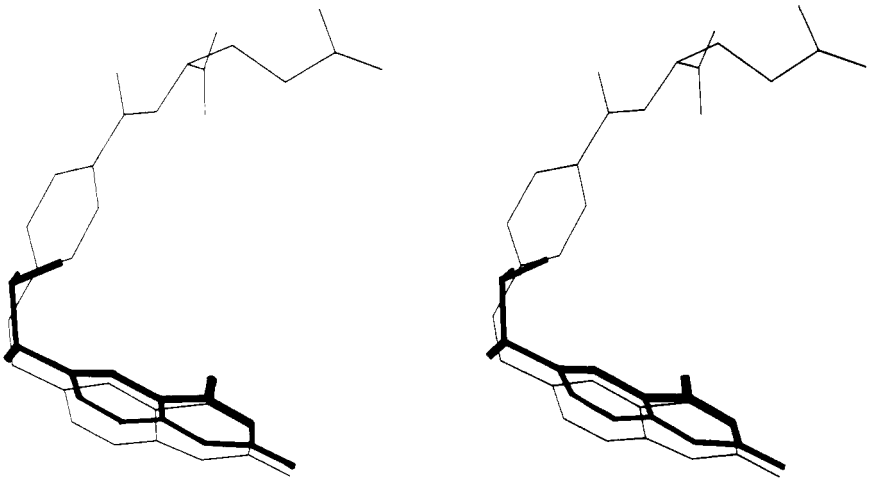

FIGURE 6: Superposition of the coordinates of biopterin from the chicken liver DHFR·NADP$^+$·biopterin complex structure (thick lines) and folate (thin lines) from the human DHFR·folate complex structure (Davies et al., 1990).

hydride acceptor atom (C7 pteridine). The difference between this 2.5-Å distance and the expected 3.7-Å van der Waals separation must largely account for the observed rotations of the nicotinamide and pteridine rings in ternary complexes as compared with their position in binary complexes. Whereas we previously proposed that progress toward the transition state would involve movement of the pteridine ring alone, the above observations suggest that movement of the cofactor nicotinamide ring is also involved. An overlap of the binding sites for the nicotinamide and pteridine rings is also indicated by the shorter than van der Waals separations between these rings within the ecDHFR·NADP$^+$·folate and cDHFR·NADP$^+$·biopterin complex structures. While the predicted van der Waals separation between C4 of the nicotinamide of NADP$^+$ and C7 of an oxidized pteridine ring is 3.6 Å, the separation between these atoms is only 3.1 Å in the ecDHFR·NADP$^+$·folate structure and 3.3 Å in the cDHFR·NADP$^+$·biopterin structure.

Effect of pABG. Although the above comparisons suggest that the binding of the pABG group of folate is not necessary to correctly position the pteridine ring in ground-state ternary complexes, it is evident that the pABG group has an important influence on catalysis by DHFR as dihydrofolate is a much better substrate than dihydropteridines with aliphatic substituents as C6. In the case of cDHFR at pH 6.8, the steady-state rate (k_{cat}) for dihydrobiopterin reduction is approximately 50% of that for dihydrofolate reduction, and the K_m for dihydrobiopterin is 2.7×10^{-6} M compared with 6.0×10^{-7} M for dihydrofolate [calculated from Kaufman (1967) and Kaufman and Gardiner (1966)]. While the greater affinity (lower K_m) for dihydrofolate can be attributed to the many nonpolar, hydrogen-bonding, and ionic interactions the pABG group makes with DHFR, an explanation for the effect on k_{cat} is less obvious. Although pre-steady-state kinetic measurements on the reduction of dihydrofolate by human (Appleman et al., 1990) and mouse (Thillet et al., 1990) DHFR have shown that hydride transfer is not rate-limiting for these vertebrate DHFRs, hydride transfer may be rate-limiting for pteridine substrates lacking a pABG group. Theoretical evidence that the pABG moiety contributes to catalysis comes from quantum-mechanical calculations which predict that the binding of the pABG group to the enzyme polarizes the folate molecule. This polarization results in a depletion of double-bond character at the C7–N8 bond for folate and the C6–N5 bond for dihydrofolate, as is expected to occur in their respective transition states (Bajorath et al., 1991a,b). Since the biopterin dihydroxypropyl group is unable to make the charge–charge interactions with DHFR that the pABG glutamate makes, such a polarization toward the transition state would not occur for biopterin.

However, aside from polarization effects, what are the geometrical effects of pABG binding? Comparison of the vacant pABG binding site of the biopterin complex with the occupied pABG site in the hDHFR·folate structure reveals that, although no large backbone rearrangements occur upon pABG binding, the binding crevice does close down somewhat on the pABG group. In hDHFR, the pABG binds in a crevice formed by residues 31–35 of αB on one side and residues 59–70 (which includes the two tight turns of residues 61–64 and 67–70) on the other. The most significant difference between the α-carbon positions of these residues in the two complexes is a 1.4 Å rms movement in the Cα positions of residues 61–64, such that the separation between this tight turn and αB is smaller in the folate complex. Because the side-chain amide of N64 hydrogen-bonds to the pABG benzoyl group in the hDHFR·folate structure, it is likely that this tight turn moves toward the pABG benzoyl and αB when folate binds to chicken DHFR as well. The difference in positions could, however, be due to crystal contacts involving K63 and N64 in the chicken DHFR crystals.

Although the backbone of αB does not appear to move upon pABG binding, differences in the position of the side chain of αB residue 31 (tyrosine in cDHFR, phenylalanine in all other known sequences of vertebrate DHFRs) in the cDHFR·NADPH, cDHFR·NADP$^+$·biopterin, and hDHFR·folate complexes provides a clue as to how pABG-induced conformational changes in this side chain may influence the binding of pteridines. In vertebrate DHFRs, pteridine substrates probably enter and depart the catalytic site via a large opening between the side chains of L22 and residue 31 (Figure 7). Since known van der Waals radii predict that atoms of L22 and Y31 should be separated by at least 7.2 Å (Bondi, 1964) for a pteridine ring to fit between them and as the separation between these residues is 7.8 Å in the cDHFR·NADPH holoenzyme complex structure, a pteridine ring should be able to diffuse into its binding site in this complex. When a pteridine ring binds, as seen in the cDHFR·NADP$^+$·biopterin complex structure, a hydrophobic interaction with the pteridine stabilizes a conformation of Y31 (Y31b) that is rotated 60° about the Cα–Cβ bond from its position in the holoenzyme (Y31a). This 60° rotation causes the side chain of Y31 to be situated closer to the side chain

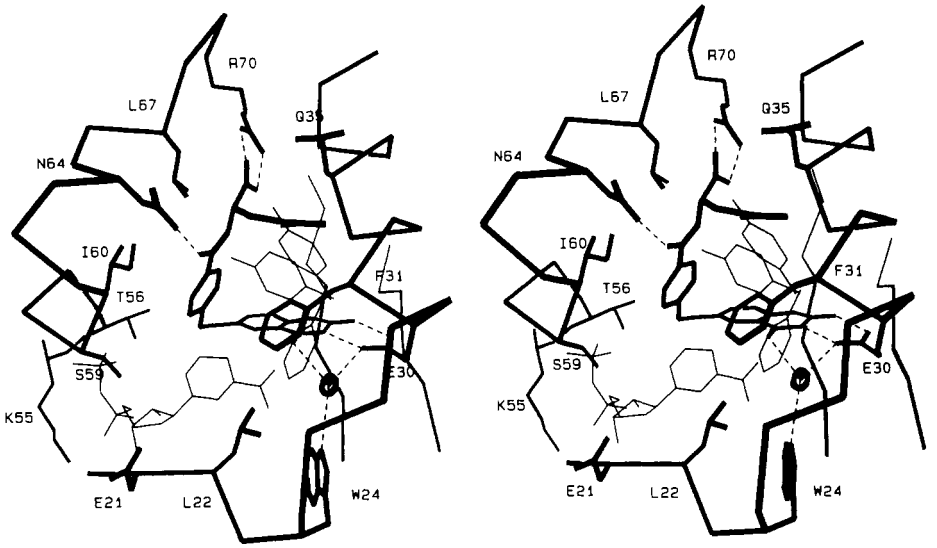

FIGURE 7: Folate binding site of molecule 2 in the structure of human DHFR complexed with folate (Davies et al., 1990). Hydrogen bonds are depicted as dashed lines, and water molecules are depicted as spheres. The side chain of F31 of molecule 1 of this structure as well as the positions of Y31a and Y31b in the cDHFR·NADP$^+$·biopterin complex structure are depicted by thin lines. The positions of the nicotinamide mononucleotide and pyrophosphate groups of NADP$^+$ in the cDHFR·NADP$^+$·biopterin complex are also depicted by thin lines.

of L22 so that the separation between these side chains closes down somewhat to 5.6 Å. This constriction in the opening to the pteridine binding site could help to keep the substrate from dissociating before reduction occurs. The observation of two positions for Y31 in the biopterin complex, however, suggests that this side chain is flexible. Biopterin could, therefore, dissociate from the enzyme when the side chain is in the Y31a position. Next, on comparing the two molecules in the asymmetric unit of the hDHFR·folate crystals, one sees that the side chain of F31 occupies two slightly different positions (Figure 7) which are separated from the side chain of L22 by 3.3 Å (molecule 1) or 4.3 Å (molecule 2). Thus, the presence of the pABG moiety of folate apparently favors an orientation of residue 31 that is still closer to L22 since in most other orientations, including Y31a and Y31b in the cDHFR·NADP$^+$·biopterin structure, the benzene ring of the side chain would sterically interfere with the pABG group.

The reality of such a conformational change in the side chain of Y31 on dihydrofolate binding to the holoenzyme is supported by the results of Kumar et al. (1981) which showed that the binding of dihydrofolate to the holoenzyme complex protects Y31 in cDHFR from reaction with benzenesulfonyl fluoride. Furthermore, a link between the pABG group, residue 31, and substrate binding was revealed by mutation of F31 of hDHFR to a leucine (the corresponding residue in *E. coli* and *L. casei* DHFR). This mutant exhibited a 67-fold decrease in the K_D for dihydrofolate, as compared to the wild-type enzyme, while the K_D for dihydrobiopterin was virtually unaffected (Tsay et al., 1990). Therefore, a pABG-induced conformational change of residue 31 of vertebrate DHFRs may partially account for the higher affinity of these enzymes for dihydrofolate as compared with dihydrobiopterin.

Thus, by favoring a conformation in which the opening to the pteridine binding site is essentially closed, the pABG group probably increases the likeihood that dihydrofolate will react before it can dissociate from the enzyme. However, while constricting the opening to the pteridine binding site will decrease substrate dissociation, it will likewise inhibit tetrahydrofolate dissociation. The benefit of inhibiting substrate dissociation may outweigh the disadvantage of inhibiting product dissociation as, under physiological conditions, dihydrofolate binding to the holoenzyme complex has been shown to be rate-limiting for human DHFR (Appleman et al., 1990). However, because it appears that a conformational change in residue 31 will be required for tetrahydrofolate to leave the enzyme, the relative ease with which this residue undergoes conformational changes may be crucial in limiting its inhibitory effect on tetrahydrofolate dissociation.

As residue 31 is positioned at the opening to the pteridine binding site and is in van der Waals contact with the pteridine ring, the precise positioning of the side chain of this residue could influence substrate protonation as well as substrate binding and product release. Small deuterium isotope effects on the burst phase of product formation in vertebrate DHFRs have suggested that an obligatory isomerization of the ternary substrate complex partially limits product formation. Such an isomerization may involve a conformational change in Y31 that exposes N5 of the dihydropteridine ring to protonation by solvent (discussed further in the next section). It is intriguing that the rate of hydride transfer is at least 30-fold slower in cDHFR than other vertebrate DHFRs which have a phenylalanine at this position and that the rate of the obligatory isomerization is also at least 8-fold lower for the chicken enzyme (Beard et al., 1989). Model-building studies on the hDHFR·folate structure reveal that a hydroxyl group added to C4 of the phenyl ring of F31 would not sterically interfere or hydrogen-bond with any other atom in this structure or appear to inhibit conformational changes of this residue. However, the possibility that the larger tyrosine may undergo conformational changes more slowly than phenylalanine cannot be ruled out.

Conformational changes in residues at the opening to the pteridine binding site have also been observed in ecDHFR (Bystroff et al., 1990). The loop of residues 16–20 (the Met-20 loop) in ecDHFR, structurally equivalent to residues 18–22 in vertebrate DHFRs, is disordered in both the apo and ecDHFR·NADP$^+$ structures but is ordered in the ecDHFR·NADP$^+$·folate structure. This loop may perform the same function in ecDHFR as residue 31 in vertebrate DHFRs, since when it becomes ordered in the ternary complex the opening to the pteridine binding site between the side chains of M20 and L28 (equivalent to residue 31 in vertebrate DHFRs) is partially closed. The separation between the side chains of M20 and L28 in the ecDHFR·NADP$^+$·folate complex is 5.0

Å. It is interesting that in all vertebrate DHFR structures the corresponding loop is ordered and it is residue 31, on the opposite side of the pteridine site opening, that assumes varying conformations while in ecDHFR it is the Met-20 loop which is mobile while L28 occupies the same position in all the structures.

Role of E30 and Water-756 in Substrate Protonation. Reduction of the N5–C6 double bond of dihydropteridine substrates is thought to occur by a mechanism involving protonation of N5 and either concomitant or subsequent hydride transfer to C6 (Huennekens & Scrimgeour, 1964; Gready, 1985; Morrison & Stone, 1988). While it is known that the 4-*pro-R* hydrogen is transferred directly from C4 (dihydrofolate) (Charlton et al., 1979), the mechanism of N5 protonation remains obscure. The glutamate side chain of E30, the sole acidic residue in the pteridine binding site, is thought to be involved in protonation of N5. Mutation of the analogous residue in ecDHFR (D27) to either asparagine or serine results in greatly diminished activity toward dihydrofolate at pH 7 but activity comparable to native ecDHFR at pH values sufficiently low to protonate dihydrofolate in solution (Howell et al., 1986). As Figures 3 and 4 show, however, the carboxylate of E30 is too far from N5 for direct protonation to occur. On the basis of the premise that this acidic group facilitates, protonation of N5, various mechanisms for proton shuttling between E30 and N5 have been proposed (Morrison & Stone, 1988; Uchimaru et al., 1989; Bystroff et al., 1990). Each of these mechanisms involves enolization of the pteridine O4 keto group aided by proton transfer to O4, via water-230, from the side chain of E30. Ab initio calculations predict that the enol forms of 6-methyl-7,8-dihydropterin are less stable than the keto form normally present in solution by only 1.4 kcal/mol or less, so this enolization is plausible (Uchimaru et al., 1989). However, as previously reported structures of DHFR do not contain any group capable of transferring a proton from O4 to N5, it was unclear how this final transfer took place.

Some authors have proposed that the lone pair on N5 abstracts the proton from the enol form of O4 directly (Morrison & Stone, 1988; Uchimaru et al., 1989), while we have argued that the transfer occurs by way of a transiently-bound water molecule hydrogen-bonded to both the O4 enol and N5 (Bystroff et al., 1990). We believe that proton transfer from E30 to N5 via O4 and an intervening water molecule is more likely for several reasons. First, the geometry between O4 and N5 is not favorable for proton transfer. We have constructed models of the enol tautomer using an O–H bond length of 1.0 Å, C4–O4–H angles of between 109 and 120°, and the O4–H bond coplanar with the pteridine ring. In these models, the O4–H–N5 angle is 92–109°, and the N5 to H distance is 2.4–2.6 Å, while in small-molecule structures, both from X-ray and from neutron diffraction studies, the average hydrogen-bond angle is 161° and the acceptor N to donor H distance is 1.9 Å (Power et al., 1973; Olovsson & Jönsson, 1976; Baker & Hubbard, 1984). Second, a water molecule that makes ideal hydrogen bonds to O4 and N5 can be modeled into both the hDHFR·folate and the ecDHFR·$NADP^+$·folate structures with very slight repositionings of F31 or M20, respectively. Finally, the cDHFR·$NADP^+$·biopterin structure reported here contains a water molecule, water-756, which forms just such a hydrogen-bonded link between O4 and N5 and which is the terminal water of a solvent chain leading to the protein surface.

The presence of water-756 in a ternary biopterin complex but not in a binary or ternary complex with folate has a simple explanation. In addition to formation of hydrogen bonds to both O4 and N5 of the pteridine, water-756 is also hydrogen-bonded to both hydroxyls of the biopterin dihydroxypropyl tail. These hydrogen bonds are not possible with folate as the ligand. The additional stabilization these hydrogen bonds provide is apparently of sufficient magnitude to order this water molecule enough to be crystallographically observable in the biopterin complex. Another reason for the appearance of this water in the biopterin complex but not in the folate complexes is that in the folate complexes N5 (pteridine) is more shielded from the bulk solvent by hydrophobic residues (L22 and F31 in the hDHFR·folate structure, M20 and L28 in the ecDHFR·$NADP^+$·folate structure). We have previously pointed out that while a water molecule transiently hydrogen-bonded to N5 may be necessary for protonation of this nitrogen, *strongly* binding a water in this position *after* protonation occurs would stabilize the positive charge on N5, instead of on C6 as required in the transition state. If, however, this water molecule were to be displaced after protonation of N5, the restored hydrophobic environment around N5 would encourage positive charge buildup at C6, which should in turn facilitate the transfer of a hydride from C4 of the nicotinamide to C6. To summarize, therefore, we propose that small conformational changes in residue 31 of vertebrate DHFRs or in M20 of ecDHFR assist in transiently binding a water molecule for protonation of N5 and then displacing this water to allow for positive charge buildup at C6 in the transition state.

ACKNOWLEDGMENT

We thank Dr. Nguyen-Huu Xuong for use of his Multiwire Data Collection facility, Dr. David Matthews for helpful discussions, and the San Diego Supercomputer Center for a generous grant of computer time.

REFERENCES

Abelson, H. T., Spector, R., Gorka, C., & Fosburg, M. (1978) *Biochem. J. 171*, 267–278.

Anderson, D. H. (1987) Ph.D. Thesis, University of California, San Diego, La Jolla, CA.

Andrews, J., Fierke, C. A., Birdsall, B., Ostler, G., Feeney, J., Roberts, G. C. K., & Benkovic, S. J. (1989) *Biochemistry 28*, 5743–5750.

Appleman, J. R., Beard, W. A., Delcamp, T. J., Prendergast, N. J., Freisheim, J. H., & Blakely, R. L. (1990) *J. Biol. Chem. 265*, 2740–2748.

Bajorath, J., Kitson, D. H., Fitzgerald, G., Andzelm, J., Kraut, J., & Hagler, A. T. (1991a) *Proteins: Struct., Funct., Genet. 9*, 217–224.

Bajorath, J., Kraut, J., Li, Z., Kitson, D. H., & Hagler, A. T. (1991b) *Proc. Natl. Acad. Sci. U.S.A. 88*, 6423–6426.

Baker, E. N., & Hubbard, R. E. (1984) *Prog. Biophys. Mol. Biol. 44*, 97–179.

Beard, W. A., Appleman, J. R., Delcamp, T. J., Freisheim, J. H., & Blakely, R. L. (1989) *J. Biol. Chem. 264*, 9391–9399.

Blakely, R. L. (1984) in *Folates and Pterins* (Blakley, R. L., & Benkovic, S. J., Eds.) Vol. 1, pp 191–253, John Wiley & Sons, New York.

Bolin, J. T., Filman, D. J., Matthews, D. A., Hamlin, R. C., & Kraut, J. (1982) *J. Biol. Chem. 257*, 13650–13662.

Bondi, A. (1964) *J. Phys. Chem. 68*, 441–451.

Bowers, S. A., & Duch, D. S. (1988) *Anal. Biochem. 172*, 169–175.

Bystroff, C., & Kraut, J. (1991) *Biochemistry 30*, 2227–2239.

Bystroff, C., Oatley, S. J., & Kraut, J. (1990) *Biochemistry 29*, 3263–3277.

Charlton, P. A., Young, D. W., Birdsall, B., Feeney, J., & Roberts, G. C. K. (1979) *J. Chem. Soc., Chem. Commun. 706*, 922–924.
Cork, C., Fehr, D., Hamlin, R., Vernon, W., Xuong, N., & Perez-Mendez, V. (1973) *J. Appl. Crystallogr. 7*, 319–323.
Davies, J. F., II, Delcamp, T. J., Prendergast, N. J., Ashford, V. A., Freisheim, J. H., & Kraut, J. (1990) *Biochemistry 29*, 9467–9479.
Dempsey, S. (1987) *Molecular Modeling System (MMS)*, Department of Chemistry Computer Facility, University of California, San Diego, La Jolla, CA.
Fierke, C. A., Johnson, K. A., & Benkovic, S. J. (1987) *Biochemistry 26*, 4085–4092.
Filman, D. J., Bolin, J. T., Matthews, D. A., & Kraut, J. (1982) *J. Biol. Chem. 257*, 13663–13672.
Frieschein, J. H., & Matthews, D. A. (1984) in *Folate Antagonists as Therapeutic Agents* (Sirotnak, F. M., Burchall, J. J., Ensminger, W. D., & Montgomery, J. A., Eds.) Vol. 1, pp 69–131, Academic Press, Inc., Orlando, FL.
Gready, J. E. (1985) *Biochemistry 24*, 4761–4766.
Groom, C. R., Thillet, J., North, A. C. T., Pictet, R., & Gedded, A. J. (1991) *J. Biol. Chem. 266*, 19890–19893.
Hendrickson, W. A. (1981) in *Refinement of Protein Structures* (Machin, P. A., Campbell, J. W., & Elder, M., Eds.) pp 1–8, Daresbury Laboratory, Warrington, U.K.
Howell, E. E., Villafranca, J. E., Warren, M. S., Oatley, S. J., & Kraut, J. (1986) *Science 231*, 1123–1128.
Huennekens, F. M., & Scrimgeour, K. G. (1964) in *Pteridine Chemistry* (Pfleiderer, W., & Taylor, E. C., Eds.) pp 355–376, Pergamon, Oxford.
Jones, T. A. (1978) *J. Appl. Crystallogr, 11*, 268–272.
Kaufman, B. T., & Gardiner, R. C. (1966) *J. Biol. Chem. 241*, 1319–1328.
Kaufman, B. T., & Kemerer, V. F. (1977) *Arch. Biochem. Biophys. 179*, 420–431.
Kaufman, S. (1967) *J. Biol. Chem. 242*, 3934–3942.
Kaufman, S., & Fisher, D. B. (1973) in *Molecular Mechanisms of Oxygen Activation* (Hayaishi, O., Ed.) pp 285–369, Academic, New York.
Konnert, J. H. (1976) *Acta Crystallogr. A32*, 614–617.
Kraut, J., Matthews, D. A. (1987) in *Biological Macromolecules and Assemblies* (Jurnak, F. A., & McPherson, A., Eds.) Vol. 3, pp 1–72, John Wiley & Sons, New York.
Kumar, A. A., Mangum, J. H., Blakenship, D. T., & Freisheim, J. H. (1981) *J. Biol. Chem. 256*, 8970–8976.
Luzzati, V. (1952) *Acta Crystallogr. 5*, 802–810.
Matthews, D. A., Alden, R. A., Freer, S. T., Xuong, N., & Kraut, J. (1979) *J. Biol. Chem. 254*, 4144–4151.
Matthews, D. A., Bolin, J. T., Burridge, J. M., Filman, D. J., Volz, K. W., Kaufman, B. T., Beddell, C. R., Champness, J. N., Stammers, D. K., & Kraut, J. (1985a) *J. Biol. Chem. 260*, 381–391.
Matthews, D. A., Bolin, J. T., Burridge, J. M., Filman, D. J., Volz, K. W., & Kraut, J. (1985b) *J. Biol. Chem. 260*, 392–399.
Matthews, D. A., Smith, S. L., Baccanari, D. P., Burchall, J. J., Oatley, S. J., & Kraut, J. (1986) *Biochemistry 25*, 4194–4204.
Morrison, J. F., & Stone, S. R. (1988) *Biochemistry 27*, 5499–5506.
Oefner, C., D'arcy, A., & Winkler, F. K. (1988) *Eur. J. Biochem. 174*, 377–385.
Olovsson, I., & Jönsson, P.-G. (1976) in *The Hydrogen Bond* (Schuster, P., Zundel, G., & Sandorfy, C., Eds.) Vol. II, p 109, North-Holland, Amsterdam.
Power, L. F., King, J. A., & Moore, F. H. (1973) *Inorg. Nucl. Chem. Lett. 9*, 629.
Reinhard, J. F., Jr., Chao, J. Y., Smith, G. K., Duch, D. S., & Nichol, C. A. (1984) *Anal. Biochem. 140*, 548–552.
Rossman, M. G., & Argos, P. (1975) *J. Biol. Chem. 250*, 7525–7532.
Smith, G. K., Banks, S. D., Bigham, E. C. & Nichol, C. A. (1987) *Arch. Biochem. Biophys. 254*, 416–420.
Stammers, D. K., Champness, J. N., Beddell, C. R., Dann, J. G., Eliopoulos, E., Geddes, A. J., Ogg, D., & North, A. C. T. (1987) *FEBS Lett. 218*, 178–184.
Thillet, J., Adams, J. A., & Benkovic, S. J. (1990) *Biochemistry 29*, 5195–5202.
Tsay, J.-T., Appleman, J. R., Beard, W. A., Prendergast, N. J., Delcamp, T. J., Freisheim, J. H., & Blakely, R. L. (1990) *Biochemistry 29*, 6428–6436.
Uchimaru, T., Tsuzuki, S., Tanabe, K., Benkovic, S. J., Furukawa, K., & Taira, K. (1989) *Biochem. Biophys. Res. Commun. 161*, 64–68.
Volz, K. W., Matthews, D. A., Alden, R. A., Freer, S. T., Hansch, C., Kaufman, B. T., & Kraut, J. (1982) *J. Biol. Chem. 257*, 2528–2536.
Wu, Y., & Houk, K. N. (1987) *J. Am. Chem. Soc. 109*, 2226–2227.
Xuong, N., Nielson, C., Hamlin, R., & Anderson, D. H. (1985) *J. Appl. Crystallogr. 18*, 342–350.